Transposon-5 mutagenesis transforms *Corynebacterium matruchotii* to synthesize novel hybrid fatty acids that functionally replace corynomycolic acid

Kuni TAKAYAMA*†‡[1], Barry HAYES*, Martha M. VESTLING§ and Randall J. MASSEY||

*Mycobacteriology Research Laboratory, William S. Middleton Memorial Veterans Hospital, Madison, WI 53705, U.S.A., †Department of Medical Microbiology and Immunology, University of Wisconsin School of Medicine, Madison, WI 53706, U.S.A., ‡Department of Bacteriology, University of Wisconsin, Madison, WI 53706, U.S.A., §Department of Chemistry, University of Wisconsin, Madison, WI 53706, U.S.A., and ||Electron Microscope Facility, University of Wisconsin School of Medicine, Madison, WI 53706, U.S.A.

Enzymes within the biosynthetic pathway of mycolic acid (C_{60}–C_{90} α-alkyl,β-hydroxyl fatty acid) in *Mycobacterium tuberculosis* are attractive targets for developing new anti-tuberculosis drugs. We have turned to the simple model system of *Corynebacterium matruchotii* to study the terminal steps in the anabolic pathway of a C_{32} mycolic acid called corynomycolic acid. By transposon-5 mutagenesis, we transformed *C. matruchotii* into a mutant that is unable to synthesize corynomycolic acid. Instead, it synthesized two related series of novel fatty acids that were released by saponification from the cell wall fraction and from two chloroform/methanol-extractable glycolipids presumed to be analogues of trehalose mono- and di-corynomycolate. By chemical analyses and MS, we determined the general structure of the two series to be 2,4,6,8,10-penta-alkyl decanoic acid for the larger series (C_{70}–C_{77}) and 2,4,6,8-tetra-alkyl octanoic acid for the smaller series (C_{52}–C_{64}), both containing multiple keto groups, hydroxy groups and double bonds. The mutant was temperature-sensitive, aggregated extensively, grew very slowly relative to the wild type, and was resistant to the presence of lysozyme. We suggest that a regulatory protein that normally prevents the transfer of the condensation product back to β-ketoacyl synthase in the corynomycolate synthase system of the wild type was inactivated in the mutant. This will result in multiple Claisen-type condensation and the formation of two similar series of these complex hybrid fatty acids. A similar protein in *M. tuberculosis* would be an attractive target for new drug discovery.

Key words: Claisen-type condensation, corynomycolic acid, electrospray MS, electron-impact MS, transposon-5 mutagenesis, ultrathin section electron microscopy.

INTRODUCTION

Tuberculosis (TB) remains the most significant single bacterial cause of mortality and morbidity in the world today, with about 8 million new cases per year and a death rate of 2.9 million per year [1,2]. At one point in time some 20 years ago, it was considered that TB was under control and that it was a matter of time before it would be eradicated. Today this optimism has subsided. The resurgence of TB has been fuelled by the HIV/AIDS epidemic [3,4], the development of multidrug-resistant strains of *Mycobacterium tuberculosis* [5–7] and the continued use of a marginally effective BCG (Bacille Calmette–Guérin) vaccine. Current therapy for TB involves 3–6 months of treatment with various combination of drugs, including isoniazid, rifampicin, ethambutol, ethionamide and pyrazinamide [8,9]. However, strains of *M. tuberculosis* resistant to these old drugs have developed and present a major problem.

Due to the emergence of multidrug-resistant strains of *M. tuberculosis*, new drugs are needed to treat TB. One of the most attractive targets for developing new anti-TB drugs is the biosynthesis and disposition of a prominent cell wall component called the mycolic acids (C_{60}–C_{90} fatty acids) [10]. This is due to the fact that these fatty acids are required for the survival of the bacilli in the hostile environment of the macrophages due to the fact that they form an impermeable asymmetrical lipid bilayer [11]. Changes in the amount and structure of mycolic acids were shown to affect the fluidity, permeability and other physical characteristics of the membrane bilayer [12–16]. Several currently used drugs target mycolic acid biosynthesis [17–19].

The pathway to the biosynthesis of mycolic acids in *M. tuberculosis* is extremely complex, and historically has been very difficult to study [20]. Therefore we have turned to *Corynebacterium* as a model/surrogate for examining the terminal steps in the biosynthesis and disposition of structurally related, but much simpler, fatty acids called corynomycolic acids (C_{32}–C_{36} fatty acids) [20]. Others have studied the biosynthesis of mycolic acid in *Corynebacterium* in the past [21,22]. By mutagenesis of transposon-5 (Tn5) [23], we have generated a knockout mutant of *Corynebacterium matruchotii* that is unable to synthesize corynomycolic acid. Instead it produces new forms of much larger hybrid fatty acids that cause dramatic changes in its growth characteristics and morphology when compared with the wild type. We suggest that the synthesis of these novel fatty acids can be attributed to loss of control of the Claisen-type condensation step.

EXPERIMENTAL

Growth of *Corynebacterium matruchotii*

C. matruchotii A.T.C.C. 14266 was grown in brain heart infusion broth (37 g/l; Becton Dickson, Sparks, MD, U.S.A.) supplemented with yeast extract (2 g/l; Life Technologies, Paisley,

Abbreviations used: ACP, acyl carrier protein; EIMS, electron-impact MS; ESMS, electrospray MS; FAME, fatty acid methyl ester(s); KS, β-ketoacyl synthase; TB, tuberculosis; TDCM, trehalose dicorynomycolate; TMCM, trehalose monocorynomycolate; Tn5, transposon-5.

[1] To whom correspondence should be addressed: Mycobacteriology Research Laboratory, William S. Middleton Memorial Veterans Hospital, 2500 Overlook Terrace, Madison, WI 53705, U.S.A. (e-mail takayama@itis.com).

Scotland, U.K.) and 0.05 % Tween 80 at 30 °C in the incubator/shaker.

Materials

Silica gel 62, acetyl chloride, sodium borohydride, lithium aluminium hydride, SDS, palmitic acid, palmitoleic acid, kanamycin and lysozyme were purchased from Sigma (St. Louis, MO, U.S.A.). Diazomethane was generated from *N*-methyl-*N*-nitroso-*p*-toluenesulphonamide (Diazald; Sigma). Sephadex LH-20 was purchased from Pharmacia Fine Chemicals (Piscataway, NJ, U.S.A.). EZ :: TN⟨KAN-2⟩Tnp Transposome was purchased from Epicentre Technology (Madison, WI, U.S.A.). 3-Hydroxyoctadecanoic acid was purchased from Larodan AB (Malmo, Sweden). [1-^{14}C]Palmitic acid (60 mCi/mmol) was purchased from Amersham (Piscataway, NJ, U.S.A.). Sodium [1-^{14}C]acetate (57 mCi/mmol) was purchased from American Radiolabelled Chemicals, Inc. (St. Louis, MO, U.S.A.). All other chemicals used in this study were reagent grade.

Analytical methods

For normal-phase TLC, silica gel GHL plates (250 μm; Analtech, Inc., Newark, DE, U.S.A.) were used with solvent A [light petroleum (b.p. 35–60 °C)/diethyl ether, 7:1 (v/v)] to separate fatty acid methyl esters (FAME), or with solvent B [chloroform/methanol/conc. ammonium hydroxide, 40:10:1 (by vol.)] to separate trehalose monocorynomycolate (TMCM) and trehalose dicorynomycolate (TDCM). For reverse-phase TLC, silica gel uniplate HPTLC-RP18 (Analtech, Inc.) was used with solvent C [chloroform/methanol, 2:3 (v/v)] to separate radioactive FAME according to size. For argentation-TLC, silica gel GHL plates were soaked in 10 % silver nitrate in acetonitrile for 60 min and dried overnight. The plates were then heated at 150 °C for 30 min (activation) and cooled. The eluting solvent for the separation of saturated and unsaturated FAME was chloroform. For the detection of bands on normal-phase TLC, plates were sprayed with 0.6 % potassium dichromate in 10 M sulphuric acid and charred. Orcinol ferric chloride spray reagent (Sigma) was used to detect glycolipids. Well characterized TMCM, TDCM and methyl corynomycolate TLC standards were synthesized previously and prepared from *C. matruchotii* and *Corynebacterium diphtheriae* A.T.C.C. 27010 [24,25]. HPLC-purified methyl α-mycolate was obtained from *Mycobacterium tuberculosis* H37Ra [26].

Preparation of electrocompetent cells

Four 200 ml cultures of *C. matruchotii* were grown at 30 °C with shaking until the absorbance at 650 nm reached approx. 0.9. The cells were harvested by centrifugation at 4550 ***g*** for 15 min at 4 °C. The well-drained pellet was washed three times with 100 ml/wash of ice-cold 10 % (v/v) glycerol. A 1 ml aliquot of ice-cold 10 % glycerol was added to this final pellet, followed by mixing, and then 100–200 μl aliquots of the suspension were transferred into Nalgene cryogenic vials (Nalge Company, Rochester, NY, U.S.A.), and stored at − 70 °C until used. Each batch was tested for viability.

Transposon mutagenesis of *C. matruchotii* by electroporation

To a 0.2 cm electroporation cuvette were added 50 μl of electrocompetent cells of *C. matruchotii* and 1 μl of EZ :: TN ⟨KAN-2⟩Tnp Transposome, and electroporation was performed using the Electroporator II, version B (Invitrogen, Carlsbad, CA, U.S.A.). This reagent is a stable synaptic complex formed between the hyperactive Tn5 transposase and the Tn5-derived transposon [23]. The conditions of electroporation were as follows: voltage, 2.0 kV; current, 25 mA; capacitance, 50 μF; resistance, 500 Ω. After electroporation, 1.0 ml of culture medium was added, followed by incubation at 30 °C for 4 h to allow the cells to recover from shock.

Selection of kanamycin-resistant mutants

The electroporated cells were diluted 1:10, 1:100 or 1:1000, and plated on to agar plates containing the culture medium and kanamycin at 10 μg/ml. After 7 days of incubation at 30 °C, colonies of kanamycin-resistant mutants of diameter 0.3–2.0 cm had developed (approx. 240 colonies/plate) in the 1:100 dilution plates. We determined that 3.3×10^4 kanamycin-resistant colonies were generated.

Selection of mutants unable to synthesize corynomycolic acid

These master plates were then replica-plated. To each master plate of the 1:100 dilution was added 450 μCi (in 0.9 ml of water) of sodium [1-^{14}C]acetate solution, followed by incubation at 30 °C for 24 h. We selected approx. 150 colonies on the master plates that were smaller than the average size, indicating slow growth. The individual colonies were numbered, hand picked and transferred into 12 ml conical centrifuge tubes containing 1.0 ml of 2 M KOH. These tubes were incubated at 56 °C for 2 h [to release the non-esterified ('free') fatty acids]. The mixtures were acidified, 2.5 ml of chloroform/methanol (2:1, v/v) was added, and then they were vortexed thoroughly and centrifuged at 3500 ***g*** for 10 min. The lower organic layers were recovered and dried. These extracts were methylated with diazomethane and analysed by radio-TLC using silica gel and solvent A. A Storm 860 Phosphorimager (Molecular Dynamics, Sunnyvale, CA, U.S.A.) was used to detect the radioactive methyl corynomycolate and FAME. We isolated 14 mutants that were completely deficient in the synthesis of corynomycolic acid. We selected several of the more prominent of these and designated them EP/2/20, EP/2/23, EP/2/38, EP/2/45 and EP/2/49. We randomly selected the mutant EP/2/23 for our study, and it was propagated in culture medium containing kanamycin at 10 or 25 μg/ml.

Chloroform/methanol extraction of mutant EP/2/23

A freshly harvested cell pellet of *C. matruchotii* EP/2/23 was extracted three times with 10 vol. of chloroform/methanol (2:1, v/v), and the extracts were pooled, filtered and dried. This fraction contained the glycolipids (including the TMCM and TDCM analogues). The residue fraction was saved for the preparation of the cell wall fraction.

Preparation of cell wall-derived fatty acids

The chloroform/methanol-extracted cells were suspended in 5 vol. of 1 % SDS, incubated at 100 °C for 30 min, centrifuged at 3500 ***g*** for 10 min, and the yellow supernatant was discarded. This treatment was repeated twice and the final white pellet was washed with ethanol (to remove residual SDS) and water. Then 2 vol. of 2 M KOH was added, and the mixture was incubated at 56 °C for 60 min, cooled, acidified with 6 M HCl and extracted with 5 vol. of chloroform/methanol (2:1, v/v). After centrifugation

at 3500 ***g***, the lower organic layer (containing the non-esterified fatty acids) was recovered, filtered and dried. This sample was methylated with diazomethane and submitted to analysis by TLC and column chromatography.

Pulse labelling of mutant EP/2/23 with [^{14}C]palmitic acid and [^{14}C]acetate to prepare radiolabelled double-band FAME

To a 200 ml culture of the *C. matruchotii* EP/2/23 mutant with an absorbance at 650 nm of 1.10 was added 144 μCi of [1-^{14}C]palmitic acid, followed by incubation in the incubator/shaker at 30 °C for 2 h. The cells were harvested by centrifugation at 4550 ***g***, washed with PBS, ethanol and acetone, and dried (yield 249.7 mg). The dried cells were wetted and extracted five times with 5 ml portions of chloroform/methanol (2:1, v/v). The organic extract was set aside. The chloroform/methanol-extracted cells were treated with 1 % SDS, saponified with 2 M KOH and processed as described above to yield the radiolabelled double-band FAME (45.3 mg; 10.8×10^6 d.p.m.). This sample was used to determine the distribution of the radioactivity between the upper and lower double-band fatty acids. It was also used to test the effectiveness of the separation of the two components of the double-band FAME by Sephadex LH-20 column chromatography.

To a 200 ml culture of mutant EP/2/23 with an absorbance at 650 nm of 0.9–1.0 was added 1.0 mCi of sodium [1-^{14}C]acetate, followed by incubation in the incubator/shaker at 30 °C for 60 min. The cells were harvested by centrifugation at 4550 ***g*** and processed in a similar manner as in the [^{14}C]palmitic acid labelling experiment (see above). The final product (cell wall FAME) had a dry weight of 12.4 mg and a radioactivity of 10.4×10^6 d.p.m. This sample was used to estimate the size of the double-band FAME by reverse-phase TLC.

Sephadex LH-20 column chromatography of the double-band FAME

A 1.8 cm × 139 cm Sephadex LH-20 column was packed as slurry in chloroform/methanol (4:1, v/v). A 2.5 cm column of sand was placed at the top to prevent the column from floating. The radioactive sample (44.4 mg; 7.6×10^6 d.p.m.) was dissolved in 2.0 ml of chloroform/methanol (4:1, v/v), applied to the column and eluted with the same solvent. The first 50 ml was collected and discarded. Then the column was placed on a fraction collector to collect 3.0 ml fractions. Analytical TLC was performed on the column fractions using silica gel plates and solvent A. The radioactivity profile was determined.

Large-scale preparation and purification of FAME from the cell wall fraction of EP/2/23

Cells of EP/2/23 from a 15.5 litre culture were harvested by centrifugation at 4550 ***g***, and washed with PBS, ethanol and acetone to yield 23.2 g of acetone-dried powder. The cell wall fraction and FAME from this fraction were prepared as described above. The entire sample of the cell wall FAME was dissolved in 35 ml of light petroleum (b.p. 35–60 °C) and applied to a 3 cm × 34 cm silica gel 62 column equilibrated in the same solvent. The elution schedule in a stepwise gradient was as follows: (a) 250 ml of light petroleum, (b) 250 ml of light petroleum/diethyl ether (99:1, v/v), (c) 500 ml of light petroleum/diethyl ether (95:5, v/v), and (d) 800 ml of light petroleum/diethyl ether (9:1, v/v). Fractions of 10 ml were collected and analysed by TLC on a silica gel plate with solvent A. The double-band FAME peak appeared in the 9:1 (v/v) solvent fractions. This ester peak was pooled, dried and weighed (107.6 mg). Analytical TLC showed this preparation to contain only the double-band FAME.

The upper and lower bands of the purified double-band FAME were separated on a Sephadex LH-20 column as described above. The initial sample load was 40–50 mg in 3 ml of chloroform/methanol (4:1, v/v). The pooled fractions from the first fractionation enriched with either the upper or the lower band were recycled on the same column. This recycling step was repeated again to yield the final TLC-pure upper- and lower-band FAME species.

Acetylation and reduction of the double-band FAME

For the acetylation experiment, a drop of acetyl chloride was added to 50–100 μg of dried sample of double-band FAME, which was allowed to stand at ambient temperature for 10 min, then dried with a stream of nitrogen. These samples were dissolved in chloroform/methanol (2:1, v/v) and applied to a silica gel TLC plate for analysis using solvent A.

For the sodium borohydride reduction experiment, 50–100 μg of dried sample was dissolved in 200 μl of normal propanol, 5 mg of solid sodium borohydride was added, and the mixture was incubated at 95 °C for 30 min. The samples were extracted with chloroform/methanol (2:1, v/v), filtered and dried. Analytical TLC was performed using silica gel plates and solvent A.

For the lithium aluminium hydride reduction experiment, 100 μg of dried sample in a screw cap tube was dissolved in 0.5 ml of 1.0 M lithium aluminium hydride solution in anhydrous diethyl ether, sealed, mixed and incubated at 22 °C for 15 min. Then 2 ml of water and 5 ml of chloroform/methanol (2:1, v/v) were added and mixed. The lower organic layer was recovered, filtered and dried. This sample was subjected to analytical TLC using silica gel and solvent A.

Electron microscopy

Washed cells of *C. matruchotii* wild type and the EP/2/23 mutant underwent several stages of preparation and analysis. (i) Fixation: the samples were fixed in 2.5 % (v/v) glutaraldehyde/2.0 % (v/v) formaldehyde in 0.1 M sodium phosphate buffer, pH 7.4, at 0 °C for 2 h. Post-fixation was performed in 2.0 % (w/v) osmium tetroxide in 0.1 M sodium phosphate buffer at 22 °C for 1 h. Pellet integrity was maintained by embedding in 2 % (w/v) molten agarose at 44 °C and solidification on ice. The agarose-embedded cells were dehydrated in a graded series of ethanol at 22 °C (50–100 %, v/v). Propylene oxide was used as transition solvent. (ii) Embedding: the dehydrated cells were infiltrated and embedded using a mixture of EMbed 812/Spurr's Low viscosity resin at 1:1 (v/v) (Electron Microscopy Sciences, Fort Washington, PA, U.S.A.). Final embedding took place with full-strength resin at 65 °C for 24 h. (iii) Sectioning and analysis: ultrathin sections (70–80 nm) were collected on a Reichert–Jung Ultracut E ultramicrotome, placed on 300 mesh Cu Gilder Thin-Bar grids. The sections were post-stained in uranyl acetate and Reynold's lead citrate, and viewed at 80 kV on a Philips CM120 transmission electron microscope (FEI Corp., Eindhoven, Netherlands). Digital micrographs documenting samples were taken using a Kodak Megaplus 1.4 camera (ATM Corp., Danvers, MA, U.S.A.).

Mass spectrometry

Electrospray-ionization mass spectra were obtained with a Micromass (Beverly, MA, U.S.A.) LTC mass spectrometer. This

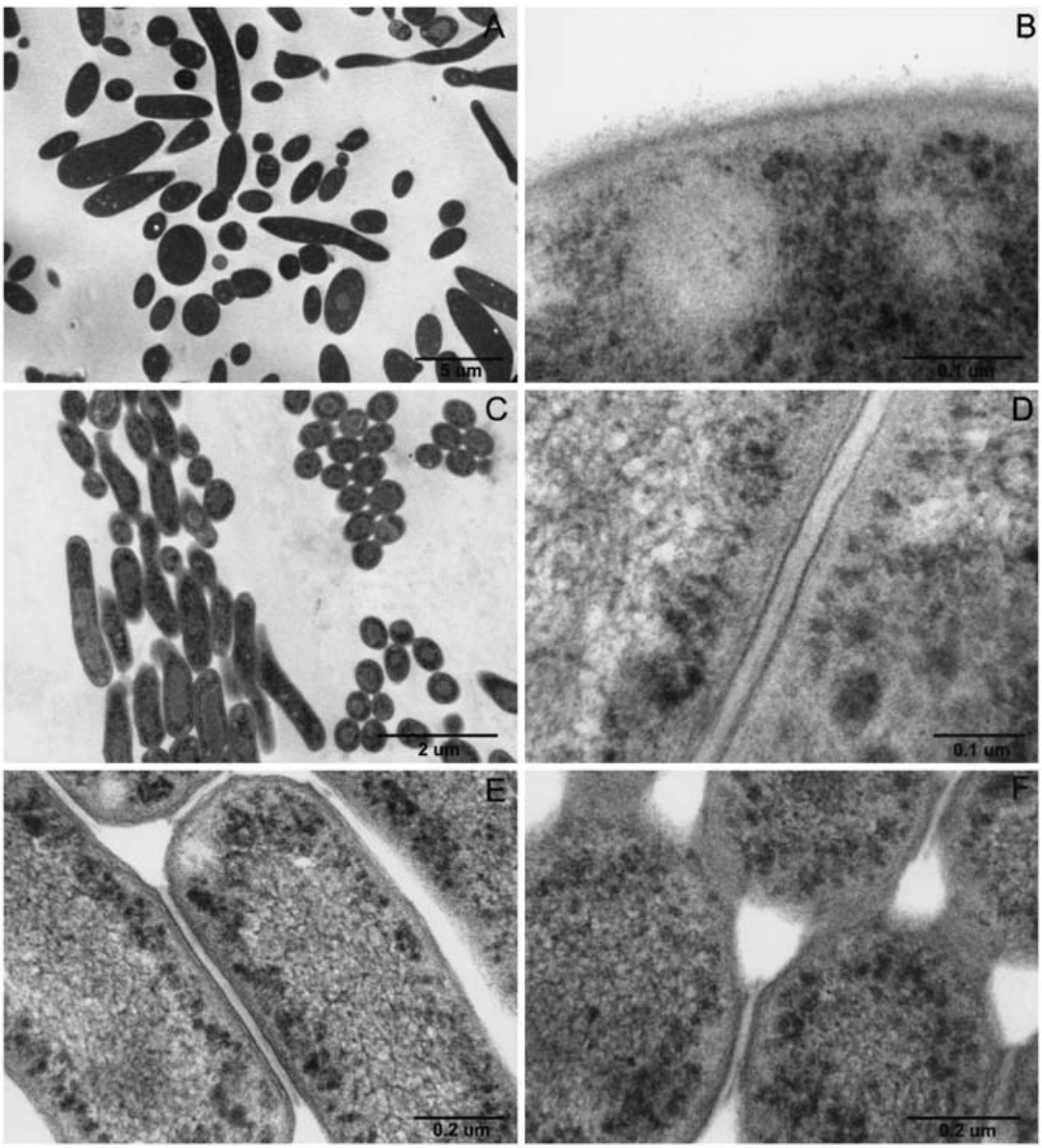

Figure 1 Ultrathin section electron micrographs of *C. matruchotii* wild type and EP/2/23 mutant

Panels (**A**) and (**B**) show wild-type cells, whereas panels (**C**)–(**F**) show the mutant. Panel (**C**) shows both horizontal (longitudinal) and vertical cross-sections, whereas (**D**) and (**E**) show horizontal cross-sections and (**F**) shows vertical cross-sections. Bars: (**A**) 5 μm, (**B**) 0.1 μm, (**C**) 2 μm, (**D**), 0.1 μm, (**E**) and (**F**) 0.2 μm.

instrument uses a time-of-flight analyser. Aliquots with added methanol were sprayed with a sample cone set at 20 V. Electron-impact mass spectra were obtained using a Micromass AutoSpec mass spectrometer. This instrument has a magnetic sector. The samples in a piece of glass capillary were inserted directly into the source and the resulting vapour was bombarded with 70 eV electrons. Perfluorokerosene was used for calibration.

RESULTS

Growth characteristics of the EP/2/23 mutant

The EP/2/23 mutant grew 2.3 times more slowly than the wild-type strain of *C. matruchotii* at 30 °C. Whereas the wild-type strain grew well at 41 °C, the EP/2/23 mutant had a non-permissive temperature of 33 °C. The wild-type strain was sensitive to the presence of lysozyme in the liquid culture medium (minimal inhibitory concentration = 1 mg/ml), whereas the EP/2/23 mutant was resistant (minimal inhibitory concentration > 30 mg/ml).

Electron microscopy of *C. matruchotii* wild type and EP/2/23 mutant

Ultrathin sections of embedded cells of *C. matruchotii* wild type and the EP/2/23 mutant were analysed by electron microscopy (Figure 1). There were four striking differences between the wild type and the mutant. The EP/2/23 mutant cells were highly aggregated, whereas the wild-type cells were well dispersed (Figures 1A and 1C). The diameter of the bacilli of the wild type was larger (1000–1500 nm) than that of the EP/2/23 mutant (380–430 nm). The outer layer identified as the cell wall in the EP/2/23 mutant appeared smaller and denser at 5 nm when

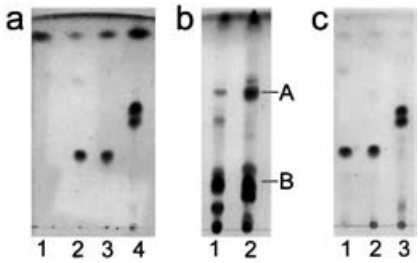

Figure 2 Silica gel TLC of FAME from *C. matruchotii* wild type and EP/2/23 mutant

(**a**) Silica gel TLC of FAME derived from whole cells after saponification. Lanes 1 and 2 contain standards of methyl palmitate and methyl corynomycolate respectively; lane 3, FAME from wild type; lane 4, FAME from EP/2/23 (10 μg each). Solvent A was used. (**b**) Silica gel TLC of chloroform/methanol (2:1, v/v) extracts of wild type (lane 1) and EP/2/23 mutant (lane 2) (100 μg each). Solvent B was used. Components A and B are orcinol-positive. (**c**) Silica gel TLC of FAME derived from the cell wall fraction of wild type (lane 2) and EP/2/23 (lane 3). Lane 1 contains methyl corynomycolate. The sample load was 10 μg, and solvent A was used. The plates were sprayed with dichromate/sulphuric acid reagent and charred.

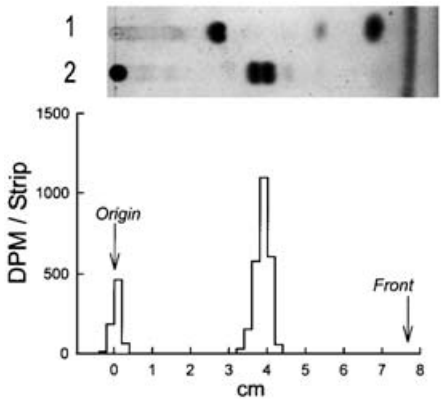

Figure 3 Distribution of radioactivity in the FAME found in the cell wall fraction after pulse labelling of the EP/2/23 mutant with [1-^{14}C]palmitic acid

TLC was performed on silica gel with solvent A. Lane 1, 10 μg of methyl corynomycolate (appearing at 2.6 cm) and 10 μg of methyl palmitate (appearing at 6.7 cm); lane 2, 30 μg (7170 d.p.m.) of FAME from EP/2/23 mutant. After spraying with dichromate/sulphuric acid reagent and performing light charring, 2.0 mm strips were scraped from the radioactive area of the plate and counted for radioactivity. The double-band ester appears at 3.5–4.2 cm.

compared with that of the wild type (wider and more diffuse at 25 nm) (Figures 1B and 1D). Points of intimate contact between the EP/2/23 cells in aggregates (especially evident in the vertical cross-sections) showed prominent accumulation of an unidentified material (Figures 1E and 1F).

Fatty acid composition of whole cells, chloroform/methanol extract and cell wall of the EP/2/23 mutant

The fatty acids derived from whole cells of the *C. matruchotii* mutant were methylated and analysed by TLC. This revealed the complete absence of methyl corynomycolate and the appearance of new 'double-band' FAME (compare lanes 2, 3 and 4 of Figure 2a). Dried cells (100 mg each) of wild type and mutant were extracted exhaustively with chloroform/methanol (2:1, v/v), and the pooled extracts were dried and weighed. The yields were 1.8 mg for the wild type and 5–6 mg for the mutant. It was confirmed by other experiments that the mutant contains much more chloroform/methanol-extractable lipid than the wild type. Examination of such a fraction from the mutant showed that the double-band fatty acids are present in two components of the chloroform/methanol extract (Figure 2b). These glycolipids could be analogues of TDCM (component A) and TMCM (component B) which are found in the wild type [27].

FAME was derived from the cell wall fraction of the EP/2/23 mutant and analysed by TLC. Figure 2(c) shows the complete absence of methyl corynomycolate and the clear presence of the new double-band FAME.

Evaluation of sizes of the double-band FAME derived from the EP/2/23 mutant

Radioactive double-band FAME was prepared from EP/2/23 cells pulse-labelled with sodium [1-^{14}C]acetate and analysed by radio-reverse-phase TLC using solvent C (results not shown). The following $R_{palmitate}$ values were obtained: methyl corynomycolate, 0.92; lower-band FAME, 0.51; upper-band FAME, 0.37. These results suggested that the upper- and lower-band FAME species are considerably larger than the methyl C_{32}-corynomycolate derived from the wild type.

Distribution of radioactivity in double-band FAME derived from the EP/2/23 mutant pulse-labelled with [^{14}C]palmitic acid

The radioactive double-band FAME derived from the EP/2/23 mutant pulse-labelled with [^{14}C]palmitic acid was analysed by TLC to determine the relative distribution of counts in the upper and lower bands. Figure 3 shows that most of the radioactivity resided in the upper band, despite the fact that the char intensities of the two bands were nearly identical. The upper band contained 1784 d.p.m., whereas the lower band contained 765 d.p.m. The upper-band/lower-band distribution of radioactivity was 2.3:1.0. This distribution, favouring the larger component, suggested that these large double-band fatty acids are assembled by condensation of C_{16} units rather than by further elongation of palmitic acid by fatty acid synthetase. The [^{14}C]palmitic acid appears to be added directly to preformed corynomycolic acid and lower-band fatty acid.

Analysis of double-band FAME by Sephadex LH-20 column chromatography

The radioactive double-band FAME was analysed by using a Sephadex LH-20 column (Figure 4). The elution volumes of the upper and lower bands were 138 ml and 143 ml respectively. TLC of the radioactive column fractions (Figure 4, inset) showed that partial separation of the two bands was achieved with this column. Thus complete separation is possible with this column by using the recycling mode. Using methyl α-mycolate (C_{76}), methyl corynomycolate (C_{32}) and methyl palmitate (C_{16}) as reference compounds, we obtained first-order estimates of the average sizes of the two FAME bands: approx. C_{73} for the upper band and approx. C_{67} for the lower band. We then used this column to obtain purified upper- and lower-band FAME species for mass spectral analysis.

Preparation and acetylation of highly purified upper-band and lower-band FAME

Highly purified upper- and lower-band FAME were prepared by combined silica gel column and Sephadex LH-20 column

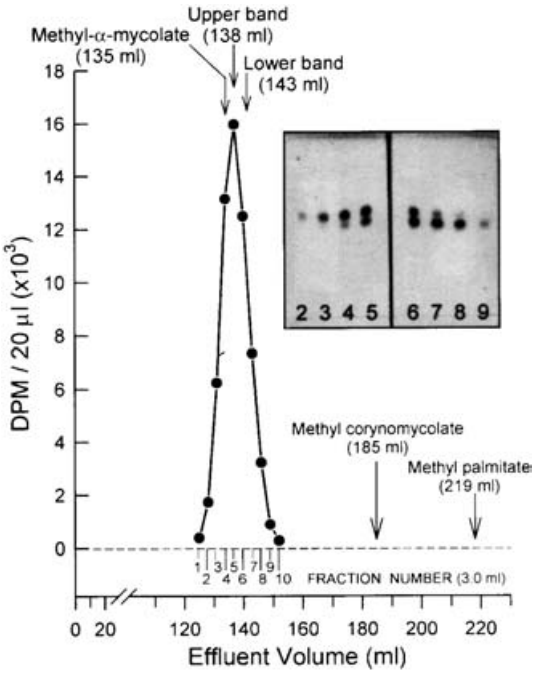

Figure 4 Sephadex LH-20 column chromatography of radiolabelled double-band FAME derived from the cell wall fraction of the *C. matruchotii* EP/2/23 mutant

The ^{14}C-labelled sample (44.4 mg; 7.6×10^6 d.p.m.) was dissolved in 2.0 ml of chloroform/methanol (4:1, v/v) and applied to a 1.8 cm × 139 cm Sephadex LH-20 column equilibrated in the same solvent. After passing 50 ml of solvent through the column, 3.0 ml fractions were collected and analysed for radioactivity and for the presence of FAME by TLC. The inset shows TLC of fractions 2–9; 2.0 μl of each fraction was applied on the silica gel plate, developed in solvent A and charred. The positions of the peaks of the upper and lower bands on the column were determined to be 138 and 143 ml effluent volumes respectively. For the purpose of size estimation, we separately established the effluent volumes of methyl α-mycolate (C_{78}), methyl corynomycolate (C_{32}) and methyl palmitate (C_{16}) on the same column.

chromatography. The purity of the two preparations was examined by analytical TLC and shown to be suitable for further analyses, including MS (results not shown).

The purified upper- and lower-band FAME were acetylated with acetyl chloride and examined by analytical TLC. Acetylation of the upper-band ester, lower-band ester, methyl 3-hydroxyoctadecanoate and methyl α-mycolate all resulted in similar increases in their mobility on normal phase TLC (results not shown). Thus both upper- and lower-band FAME contain at least one free hydroxy group.

Reduction of purified double-band FAME

Purified double-band FAME were reduced with sodium borohydride and examined by silica gel TLC using a solvent system of light petroleum (b.p. 35–60 °C)/diethyl ether (2:1, v/v) (results not shown). Before reduction, the sample gave two bands at R_F 0.92 and 0.90. After reduction, this pair showed bands at R_F 0.54 and 0.49. These results suggested that the keto groups in the double-band FAME were reduced to give the hydroxy groups.

The purified double-band FAME were also reduced with lithium aluminium hydride and examined by silica gel TLC using a solvent system of light petroleum/diethyl ether (5:1, v/v) (results not shown). Before reduction, the sample gave two bands at R_F 0.66 and 0.60. After reduction, this pair showed bands at R_F 0.19 and 0.16. In this case, both keto and carboxyl ester groups

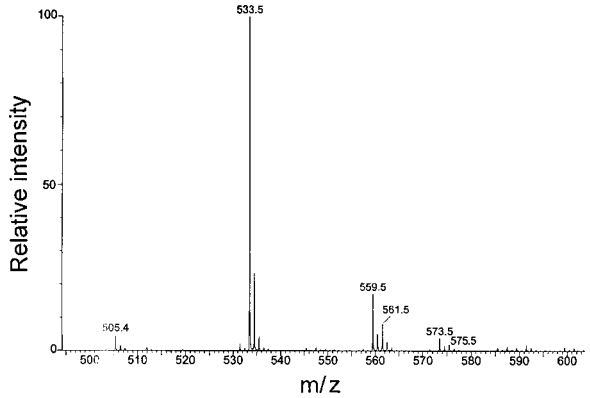

Figure 5 Partial positive ion electrospray mass spectrum of methyl corynomycolate from *C. matruchotii* wild type

This is the molecular ion region where the adduct ions are $M\text{Na}^+$.

are reduced to the hydroxy groups. Thus both the upper and lower bands of the double-band FAME contained an undetermined number of keto groups.

Presence of double bonds in upper-band and lower-band FAME

The purified upper- and lower-band FAME were analysed by argentation-TLC using chloroform as the solvent (results not shown). The reference lipids used were (saturated) methyl palmitate (R_F value of 0.83) and (monounsaturated) methyl palmitoleate (R_F 0.22). The upper-band FAME gave a complex pattern showing five bands at R_F 0.31, 0.25, 0.18, 0.14 and 0.12 (major bands underlined). The lower-band FAME gave only two bands at R_F 0.25 and 0.17. These results showed that both upper- and lower-band FAME contained multiple components based on the number and position of the double bonds. It was not possible to determine the degree of unsaturation by this method.

Electrospray MS (ESMS) and electron-impact MS (EIMS) of methyl corynomycolate from *C. matruchotii* wild type

The silica gel column-purified methyl corynomycolate from *C. matruchotii* wild type was analysed by ESMS. A prominent $M\text{Na}^+$ molecular ion peak appeared in the spectrum at m/z 533, which represented the saturated methyl C_{32}-corynomycolate (Figure 5). Much lower intensity $M\text{Na}^+$ ion peaks appeared at m/z 505 (C_{30}), 559 (unsaturated C_{34}), 561 (C_{34}), 573 (unsaturated C_{35}) and 575 (C_{35}). EIMS of methyl corynomycolate showed two fragments of $M–CH_3(CH_2)_{14}C(OH)H$ at m/z 270 and $M–CH_3(CH_2)_{14}$ at m/z 299 (results not shown). Also present were $M–H_2O$ at m/z 492 and $M–OCH_3$ at m/z 479. This established an M_r of 510 for the major component (C_{32}) in wild-type *C. matruchotii* and the presence of the characteristic 2-alkyl-3-hydroxyl functional group. These results are consistent with those of Shimakata et al. [22].

ESMS and EIMS of the upper-band FAME

The purified upper-band FAME was analysed by ESMS, and the spectrum is shown in Figure 6. It showed a series of $M\text{Na}^+$ molecular ion peaks at m/z 1119, 1132, 1147, 1161, 1175, 1189 and 1217. These peaks differed by CH_2 units (14 atomic mass

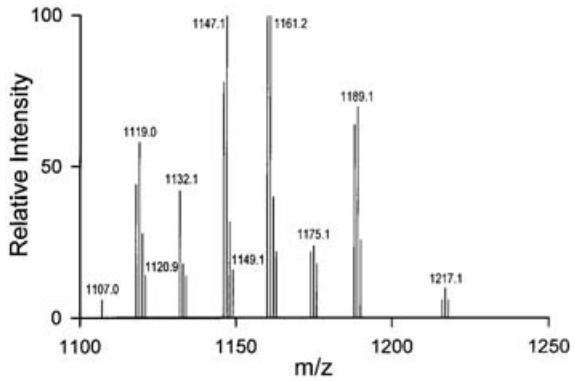

Figure 6 Partial positive ion electrospray mass spectrum of purified upper-band FAME

This is the molecular ion region where the adduct ions are MNa$^+$.

Table 1 Proposed chemical structure and molecular ions by ESMS of the related series of upper-band FAME derived from the EP/2/23 mutant

The corynomycolyl methyl ester structure is shown in bold lettering, and cleavage by EIMS gives fragment A. X represents either a keto [C=O] or a hydroxy [CH—OH] group. The numbers and positions of keto and hydroxy groups in this structure were not established. Since the wild-type corynomycolyl residue is on the left side of the structure, we can assign *a* and *b* to equal 13. Figure 6 gives the electrospray mass spectrum of related series of upper-band FAME. The major components are underlined.

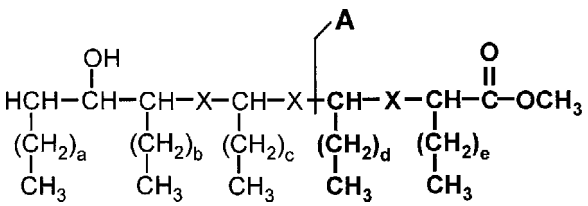

MNa$^+$	M	a–e*	Molecular formula
1119	1096	55	$C_{71}H_{146}O_6$
1132	1109	56	$C_{72}H_{148}O_6$
<u>1147</u>	1124	57	$C_{73}H_{150}O_6$
<u>1161</u>	1138	58	$C_{74}H_{152}O_6$
1175	1152	59	$C_{75}H_{154}O_6$
1189	1166	60	$C_{76}H_{156}O_6$
1217	1194	62	$C_{78}H_{160}O_6$

* The number and position of the double bond in the three hydrocarbon side chains on the right side were neither indicated by $(CH{=}CH)_n$ nor established; however, the sum of the keto group and double bond would equal 4.

units). The proposed structure of this series is given in Table 1. We suggest that it is a methyl 2,4,6,8,10-penta-alkyl decanoate containing multiple keto groups, hydroxy groups and double bonds. The combined length of the hydrocarbon chain would vary from 56 to 63 carbons ($a+1$ to $e+1$). The M_r range is from 1096 to 1194, with the major components at 1147 and 1161. EIMS of the upper-band FAME showed fragment A peaks (pyrolytic cleavage) at m/z 509, 523, 537, 551, 560, 565, 580, 594, 608, 621 and 636 (Figure 7 and Table 1). This would represent condensation by any combination of C_{16}–C_{21} fatty acids in the formation of the methyl corynomycolate moiety of the upper-band fatty acid. As the chain length increases by CH_2 units from m/z 565, other peaks are seen with decreases in size of 2 atomic mass units, indicating the presence of a keto group and/or unsaturation. The peak at

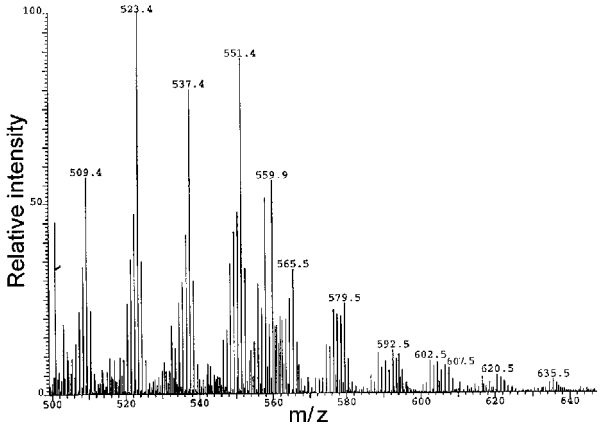

Figure 7 Partial electron-impact mass spectrum of purified upper-band FAME

Cleavage A (see Table 1) yields a series of fragments that are structurally related to methyl corynomycolate.

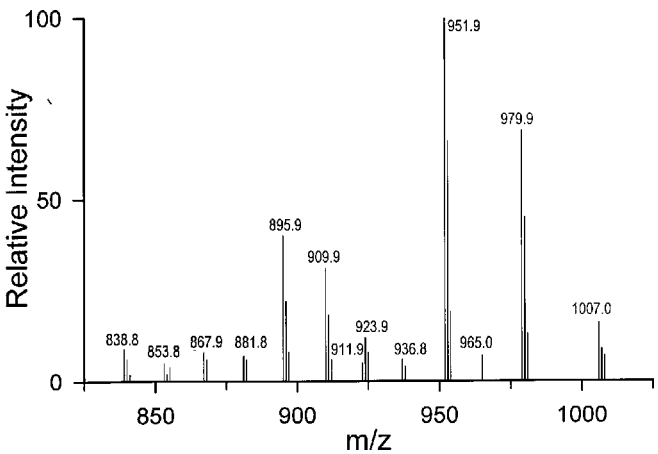

Figure 8 Partial positive ion electrospray mass spectrum of purified lower-band FAME

This is the molecular ion region where the adduct ions are MNa$^+$.

m/z 560 is a good example of this difference from m/z 565. This region does not have the fidelity of chain length and saturation seen in the corynomycolate of the wild type.

ESMS and EIMS of the lower-band FAME

The purified lower-band FAME was analysed by ESMS, and the spectrum is shown in Figure 8. It showed a series of MNa$^+$ molecular ion peaks at m/z 839, 854, 868, 882, 896, 910, 924, 937, 952, 965, 980 and 1007. These peaks differed by CH_2 units. The proposed structure of this series is given in Table 2. We suggest that it is a methyl 2,4,6,8-tetra-alkyl octanoate containing multiple keto groups, hydroxy groups and double bonds. The combined length of the hydrocarbon chain would vary from 41 to 53 carbons ($a+1$ to $d+1$). The M_r range is from 816 to 984, with the major components at 952 and 980. EIMS of the lower-band FAME gave fragment A peaks similar to those of the

Table 2 Proposed chemical structure and molecular ions by ESMS of the related series of the lower-band FAME derived from the EP/2/23 mutant

The corynomycolyl methyl ester structure is shown in bold lettering. X represents either a keto [C=O] or a hydroxy [CH−OH] group. The numbers and positions of keto and hydroxy groups in this structure were not established. Since the wild-type corynomycolyl residue is on the left side of the structure, we can assign *a* and *b* to equal 13. Figure 8 gives the electrospray mass spectrum of the related series of lower-band FAME. The major components are underlined.

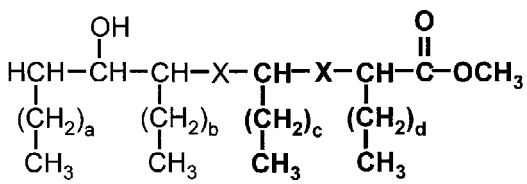

*M*Na$^+$	M	*a*–*d**	Molecular formula
839	816	40	$C_{53}H_{98}O_5$
854	830	41	$C_{54}H_{100}O_5$
868	845	42	$C_{55}H_{102}O_5$
882	859	43	$C_{56}H_{104}O_5$
896	873	44	$C_{57}H_{106}O_5$
910	887	45	$C_{58}H_{108}O_5$
924	901	46	$C_{59}H_{110}O_5$
937	914	47	$C_{60}H_{112}O_5$
952	929	48	$C_{61}H_{114}O_5$
966	943	49	$C_{62}H_{116}O_5$
980	957	50	$C_{63}H_{118}O_5$
1007	984	52	$C_{65}H_{122}O_5$

* The number and position of the double bond in the three hydrocarbon side chains on the right side were neither indicated by $(CH=CH)_n$ nor established; however, the sum of the keto group and double bond would equal 4.

upper-band FAME (results not shown). A minor series of saturated C_{81}–C_{90} esters was also detected in the lower-band FAME fraction (results not shown).

DISCUSSION

Mycolic acid is defined as α-, β-alkyl, β-hydroxyl fatty acid. *C. matruchotii* A.T.C.C. 14266 produces a small and simple version of mycolic acid which we call corynomycolic acid [20]. It is primarily a condensation product of two molecules of hexadecanoic acid (C_{16}). Thus the α-alkyl group is C_{14}, whereas the β-alkyl group is C_{15}. *M. tuberculosis* produces three related series of much larger mycolic acids [10]. In this case, the α-alkyl group is primarily C_{24} and the β-alkyl group is greater than C_{50}. The β-alkyl group contains a functional group unique to each of the three related series, i.e. *cis/trans*-cyclopropane rings, a methoxy group and a keto group. Mechanistically, the terminal anabolic steps of mycolic acids starting from Claisen-type condensation to the transfer to trehalose and to cell wall arabinogalactan should be similar in the two micro-organisms. Our objective was to study these terminal reactions in the simple *C. matruchotii* system and then relate the results to the more complex *M. tuberculosis* system. We took the genetic approach to this study, with the aim of developing a new target for drug discovery against TB.

By Tn5 mutagenesis, we have transformed *C. matruchotii* into a mutant that is unable to synthesize corynomycolic acid. Instead, it synthesizes two similar series of novel fatty acids that are structurally related to corynomycolic acid. These two new series were released from the cell wall fraction and from the two chloroform/methanol-extractable glycolipids (presumably analogues of TDCM and TMCM) of the EP/2/23 mutant by mild saponification. We then converted the non-esterified fatty acids into their methyl esters (FAME) and purified them by combined silica gel column and Sephadex LH-20 column chromatography. These samples were submitted to chemical analyses and MS. From these results, we arrived at the general structures of the two series as 2,4,6,8,10-penta-alkyl decanoic acid for the upper band (Table 1) and 2,4,6,8-tetra-alkyl octanoic acid for the lower band (Table 2), with both series containing multiple keto groups, hydroxy groups and double bonds. The numbers and positions of these groups were not established in these complex mixtures.

As shown by reverse-phase TLC and Sephadex LH-20 column chromatography, these new fatty acids were much larger than the C_{32}-corynomycolic acid found in *C. matruchotii* wild type. In fact, the fatty acids ranged in size from C_{70} to C_{77} for the upper band and from C_{52} to C_{64} for the lower band. These sizes approached that of C_{76}-α-mycolic acid of *M. tuberculosis* [26]. Thus the corynomycolic acid normally found in wild-type *C. matruchotii* covalently linked to the arabinogalactan moiety of cell wall peptidoglycan and esterified to trehalose was replaced by the novel double-band fatty acids in the EP/2/23 mutant. Because of these changes, the EP/2/23 mutant exhibited unusual growth characteristics. Ultrathin section electron microscopy revealed that the mutant cells appeared different from the wild-type cells. These differences are consistent with the presence of the novel corynomycolate hybrid fatty acids. Liu et al. [28] showed that the nature of mycolic acid plays a crucial role in determining the fluidity and permeability of the mycobacterial cell wall.

Shimakata et al. [29] reported on the current view of how *C. matruchotii* processes newly synthesized corynomycolic acid to form the cell wall arabinogalactan–corynomycolate and TDCM. In their scheme, newly synthesized corynomycolic acid is first transferred to trehalose 6-phosphate to form trehalose 6′-corynomycolyl-6-phosphate. Dephosphorylation of this product yields TMCM. This key intermediate is the donor of the corynomycolyl group to the cell wall arabinogalactan, and is the source of TDCM. For our study, we required taking a few steps backward in this pathway and examining the condensation step in the biosynthesis of corynomycolic acid. Then we proposed how these novel hybrid fatty acids might be synthesized.

We suggest that the existing corynomycolate synthase system found in wild-type *C. matruchotii* is involved in the synthesis of the novel hybrid fatty acids, as shown in Scheme 1. We further suggest that this is a fully dissociable type II system [30]. However, it is a highly structured multifunctional array in its active state. It would be similar to the type II polyketide biosynthesis system [31]. This array is composed of acyl carrier protein (ACP), β-ketoacyl synthase (KS), β-ketoacyl reductase and acyl transferase. This KS is a dedicated enzyme for the Claisen-type condensation step for the synthesis of corynomycolic acid in *C. matruchotii*. Scheme 1 shows that reaction 1 is the beginning of the aberrant pathway in the mutant. It involves the transfer of a newly synthesized corynomycolyl group as an ACP derivative back to KS by the acyl transferase enzyme. This is abnormal and does not occur in the wild type. Normally after synthesis, the corynomycolyl group is transferred directly to an acyl carrier intermediate (trehalose 6-phosphate), leading to further transfer to TMCM and cell wall arabinogalacatan. Reaction 2 is the loading step, where a hexadecanoyl group is transferred to ACP from the CoA derivative. Reaction 3 is the Claisen-type condensation step, whereby a C_{16} unit is added to the existing C_{32}-corynomycolyl–KS to form the hybrid C_{48}-corynomycolyl–ACP. The C_{32}-corynomycolate and the product of

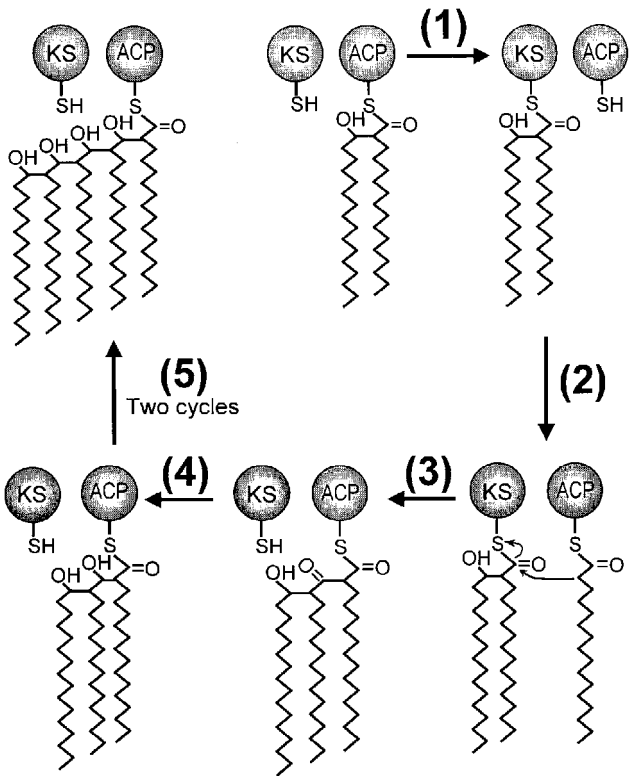

Scheme 1 Proposed pathway for the biosynthesis of novel double-band fatty acids (corynomycolic acid hybrids) in the *C. matruchotii* EP/2/23 mutant

The essential domains illustrated by circles are KS and ACP. Two other enzymes involved but not shown are acyl transferase and β-ketoacyl reductase. The five steps in this pathway are: (**1**) acyl transfer to KS, (**2**) loading ACP with an acyl group from hexadecanoyl-CoA, (**3**) Claisen-type condensation, (**4**) β-ketoacyl reduction, and (**5**) one additional cycle to yield the lower-band fatty acids or two cycles to yield the upper-band fatty acids. This is an idealized pathway for the purpose of illustration, where we show condensation of $C_{16:0}$ fatty acids and generation of fully reduced products.

this reaction do not accumulate in the EP/2/23 mutant. Reaction 4 is the reduction step, in which the keto group is reduced to the hydroxy group. This reaction might not be fully active in the mutant, as indicated by the presence of keto groups in the hybrid fatty acids. Finally, reaction 5 is a repeat of the previous reactions 1–4. One cycle of reaction 5 yields a related series of the lower-band fatty acids, and two cycles yields a related series of the upper-band fatty acids. Based on the proposed pathway given in Scheme 1, fragment A (see Table 1) is identified as the product of the final two condensation steps. The starting corynomycolate in this pathway (the substrate for reaction 1) would appear on the left side of the final product. We would expect this to be similar to the wild-type corynomycolate, i.e. essentially a saturated C_{32} fatty acid. The acyl donors for the latter reactions (final three cycles) must be a mixture of C_{16}–C_{21} fatty acids with various degrees of unsaturation. Each cycle of reactions would yield either a keto or a hydroxy group. We suggest that the final three cycles of acyl additions lead to structural variation in the related series of both upper- and lower-band FAME species.

We suggest that the regulatory protein that specifically blocks the acyl transferase (reaction 1 in Scheme 1) in the wild type has been inactivated in the EP/2/23 mutant. This results in uncontrolled Claisen-type condensation, and several cycles of these reactions yield the two related series of hybrid fatty acids. We are presently performing genetic analysis and proteomics to confirm this mechanism and to identify this protein. A similar protein that controls mycolic acid synthesis might be found in *M. tuberculosis*. It would be an attractive target for new drug discovery.

Further studies on the Tn5 mutagenesis of *C. matruchotii* should yield other interesting knockout mutants deficient in the synthesis and disposition of corynomycolic acid.

We thank William S. Reznikoff (Department of Biochemistry, University of Wisconsin, Madison, WI 53706, U.S.A.) for his valuable advice on the use of the Tn5 reagent, Hiram Sanchez for assistance in the electroporation experiments, and Kathryn Kleckner and Ben August for preparing the Figures. This work was supported by the Research Service of the Department of Veterans Affairs (K.T.), and NSF Awards CHE-9974839 and CHE-9304546 to M.M.V.

REFERENCES

1 Bloom, B. R. and Murray, C. J. L. (1992) Tuberculosis: commentary on a reemergent killer. Science **257**, 1055–1064
2 Snider, D. E., Raviglione, M. and Kochi, A. (1994) Global burden of tuberculosis. In Tuberculosis: Pathogenesis, Protection, and Control (Bloom, B. R., ed.), pp. 3–11, American Society for Microbiology, Washington, DC
3 Drobniewski, F. A., Posniak, A. L. and Uttley, A. H. C. (1995) Tuberculosis and AIDS. J. Med. Microbiol. **43**, 85–91
4 Castro, K. G. (1995) Tuberculosis as an opportunistic disease in persons infected with human immunodeficiency virus. Clin. Infect. Dis. **21** (Suppl. 1), S66–S71
5 Iseman, M. D. (1994) Evolution of drug-resistant tuberculosis. Proc. Natl. Acad. Sci. U.S.A. **91**, 2428–2429
6 Gleissberg, V. (1999) The threat of multidrug resistance: is tuberculosis ever untreatable or uncontrollable? Lancet **353**, 998–999
7 Reichman, L. B. and Tanne, J. H. (2002) Timebomb: The Global Epidemic of Multi-Drug Resistant Tuberculosis, McGraw-Hill, NY
8 Bates, J. H. (1995) Tuberculosis chemotherapy. Am. J. Respir. Crit. Care Med. **151**, 942–943
9 Friedman, L. N. (2000) Tuberculosis: Current Concepts and Treatment, 2nd edn, CRC Press, Boca Raton, FL
10 Minnikin, D. E. (1982) Lipids: complex lipids, their chemistry, biosynthesis and roles. In The Biology of the Mycobacteria, vol. 1 (Ratledge, C. and Stanford, J, eds.), pp. 95–184, Academic Press, New York
11 Liu, J., Rosenberg, E. Y. and Nikaido, H. (1995) Fluidity of the lipid domain of cell wall from *Mycobacterium chelonae*. Proc. Natl. Acad. Sci. U.S.A. **92**, 11254–11258
12 George, K. M., Yuan, Y., Sherman, D. R. and Barry, III, C. E. (1995) The biosynthesis of cyclopropanated mycolic acids in *Mycobacterium tuberculosis.* J. Biol. Chem. **270**, 27292–27298
13 Jackson, M., Raynaud, C., Laneelle, M.-A., Guilhot, C., Laurent-Winter, C., Ensergueix, D., Glcquel, B. and Daffe, M. (1999) Inactivation of the antigen 85C gene profoundly affects the mycolate content and alters the permeability of the *Mycobacterium tuberculosis* cell envelope. Mol. Microbiol. **31**, 1573–1587
14 Wang, L., Slayden, R. A., Barry, III, C. E. and Liu, J. (2000) Cell wall structure of a mutant of *Mycobacterium smegmatis* defective in the biosynthesis of mycolic acids. J. Biol. Chem. **275**, 7224–7229
15 Glickman, M. S., Cox, J. S. and Jacobs, Jr, W. R. (2000) A novel mycolic acid cyclopropane synthetase is required for cording, persistence, and virulence of *Mycobacterium tuberculosis*. Mol. Cell **5**, 717–727
16 Dubnau, E., Chan, J., Raynaud, C., Mohan, V. P., Laneelle, M.-A., Yu, K., Quemard, A., Smith, I. and Daffe, M. (2000) Oxygenated mycolic acids are necessary for virulence of *Mycobacterium tuberculosis* in mice. Mol. Microbiol. **36**, 630–637
17 Winder, F. G. and Collins, P. B. (1970) Inhibition by isoniazid of synthesis of mycolic acids in *Mycobacterium tuberculosis*. J. Gen. Microbiol. **66**, 41–48
18 Takayama, K. and Davidson, L. A. (1979) Isonicotinic acid hydrazide, In Antibiotics, vol. 1 (Hahn, F. E., ed.), pp. 98–119, Springer-Verlag, Berlin
19 Winder, F. G., Collins, P. B. and Whelan, D. (1971) Effects of ethionamide and isoxyl on mycolic acid synthesis in *Mycobacterium tuberculosis* BCG. J. Gen. Microbiol. **66**, 379–380
20 Takayama, K. and Qureshi, N. (1984) Structure and synthesis of lipids. In The Mycobacteria – A Sourcebook (Kubica, G. P. and Wayne, L. G., eds.), pp. 315–344, Marcel Dekker, New York
21 Walker, R. W., Prome, J. C. and LaCave, C. S. (1973) Biosynthesis of mycolic acids. Formation of a C_{32} β-keto ester from palmitic acid in a cell-free system of *Corynebacterium diphtheriae*. Biochim. Biophys. Acta **326**, 52–62

22 Shimakata, T., Iwaki, M. and Kusaka, T. (1984) *In vitro* synthesis of mycolic acids by the fluffy layer fraction of *Bacterionema matruchotii*. Arch. Biochem. Biophys. **229**, 329–339
23 Goryshin, I. Y., Jendrisak, J., Hoffman, L. M., Meis, R. and Reznikoff, W. S. (2000) Insertional transposon mutagenesis by electroporation of released Tn5 transposition complexes. Nat. Biotechnol. **18**, 97–100
24 Datta, A. K., Takayama, K., Nashed, M. A. and Anderson, L. (1991) An improved synthesis of trehalose 6-mono- and 6,6′-di-corynomycolates and related esters. Carbohydr. Res. **218**, 95–109
25 Datta, A. K. and Takayama, K. (1993) Biosynthesis of a novel 3-oxo-2-tetradecyldecanoate-containing phospholipid by a cell-free extract of *Corynebacterium diphtheriae*. Biochim. Biophys. Acta **1169**, 135–145
26 Qureshi, N., Takayama, K., Jordi, H. C. and Schnoes, H. K. (1978) Characterization of the purified components of a new homologous series of α-mycolic acids from *Mycobacterium tuberculosis* H37Ra. J. Biol. Chem. **253**, 5411–5417
27 Shimakata, T., Tsubokura, K., Kusaka, T. and Shizukuishi, K. (1985) Mass spectrometric identification of trehalose 6-monomycolate synthesized by the cell-free system of *Bacterionema matruchotii*. Arch. Biochem. Biophys. **238**, 497–508
28 Liu, J., Barry, C. E., Besra, G. S. and Nikaido, H. (1996) Mycolic acid structure determines the fluidity of the mycobacterial cell wall. J. Biol. Chem. **271**, 29545–29551
29 Shimakata, T. and Minatogawa, Y. (2000) Essential role of trehalose in the synthesis and subsequent metabolism of corynomycolic acid in *Corynebacterium matruchotii*. Arch. Biochem. Biophys. **380**, 331–338
30 Kremer, L., Douglas, J. D., Baulard, A. R., Morehouse, C., Guy, M. R., Alland, D., Dover, L. G., Lakey, J. H., Jacobs, Jr, W. R., Brennan, P. J. et al. (2000) Thiolactomycin and related analogues as novel anti-mycobacterial agents targeting KasA and KasB condensing enzymes in *Mycobacterium tuberculosis*. J. Biol. Chem. **275**, 16857–16864
31 Stauton, J. and Weissman, K. J. (2001) Polyketide biosynthesis: a millennium review. Nat. Prod. Rep. **18**, 380–416

Received 11 February 2003/1 April 2003; accepted 14 April 2003
Published as BJ Immediate Publication 14 April 2003, DOI 10.1042/BJ20030248